Analysis of the effect of uncertainties in hydrodynamic parameters on the accuracy of the gas flow modulation technique for bubble columns

Marchini, S.; Schubert, M.; Hampel, U.;

Originally published:

November 2021

Chemical Engineering Journal 434(2022), 133478

DOI: https://doi.org/10.1016/j.cej.2021.133478

Perma-Link to Publication Repository of HZDR:

https://www.hzdr.de/publications/Publ-32891

Analysis of the effect of uncertainties in hydrodynamic parameters on the accuracy of the gas flow modulation technique for bubble columns

Sara Marchini[a,b*], Markus Schubert[b], Uwe Hampel[a,b]

[a]Chair of Imaging Techniques in Energy and Process Engineering, Technische Universität Dresden, 01062 Dresden, Germany

[b]Institute of Fluid Dynamics, Helmholtz-Zentrum Dresden-Rossendorf, Bautzner Landstraße 400, 01328 Dresden, Germany

*Corresponding author: s.marchini@tu-dresden.de (S. Marchini)

Abstract

The gas flow modulation technique has recently been proposed as a novel method for determining the axial gas dispersion coefficient in bubble columns. The approach is based on a marginal sinusoidal modulation of the gas inlet flow rate that acts as a virtual tracer. Axial gas dispersion is then inversely calculated from amplitude damping and phase shift via an analytical solution of the axial dispersion model. The proposed study provides an analysis of the inherent uncertainties related to the assumptions of constant axial gas dispersion coefficient and bubble rise velocity, which are crucial for implementing the method. Besides, the sensitivity of the approach is assessed as function of the modulation parameters, the bubble rise velocity and the axial gas dispersion coefficient. Eventually, the possibility of tailoring the modulation parameters depending on the expected value of the axial gas dispersion coefficient to increase the sensitivity and to reduce the uncertainty is also assessed.

Keywords

Bubble columns, bubble column reactors, axial dispersion coefficient, axial dispersion model, uncertainty analysis, sensitivity analysis

1. Introduction

Gas-liquid reactors, such as bubble columns and trickle beds, are subjected to dispersion phenomena on both gas and liquid side that affect their performances, i.e. space-time yield. The term 'dispersion' summarizes both convective and diffusive phenomena, which cause deviation from plug-flow conditions. These phenomena include recirculation, stagnant areas, axial back-mixing, molecular diffusion and so on.

Many theoretical approaches have been developed to account for the effects of dispersion, of which the axial dispersion model (ADM) is the most widely used one [1]. Although the single phenomena composing dispersion are not stochastic, their combination can be fairly considered as such [1]. Based on this assumption, a diffusion-like term can be used to describe dispersion. The spatiotemporal concentration of a considered species in the liquid or gas phase can be described using the convection-diffusion equation

$$\frac{\delta c}{\delta t} = D\frac{\delta^2 c}{\delta x^2} - u\frac{\delta c}{\delta x}, \qquad 1$$

where c is the concentration of a species in the considered phase, u is the superficial velocity of the considered phase and D is the axial dispersion coefficient.

It is worth mentioning that, when applying the ADM to bubble columns, the momentum transferred between the phases is considered minimal and its effect is included in the value of the axial dispersion coefficient. On the gas side, this assumption is reasonable in bubble columns in which the liquid is supplied as a batch or the velocity of the liquid phase is low. This assumption is a characteristic of the ADM and has widely been applied in the literature (e.g., [2], [3]). However, the use of the ADM is only a simplification and comes with some criticism [1]. Thus, some authors have developed alternative models that combine the mass transfer equation with the momentum equation, deriving a kinematic and dynamic wave expression in two-phase flow (e.g., [4]). Such approaches also include a pseudo-diffusive term and, therefore, an axial dispersion coefficient. It should be noted that the present study only deals with the axial gas dispersion coefficient as defined in the ADM.

A reliable quantification of the axial dispersion coefficients on both liquid and gas sides is crucial for a performance assessment and tailored design of such contactors. Liquid dispersion coefficients have widely been measured and studied. On the contrary, only few data are available for gas dispersion coefficient [2], although the need for measuring it is generally recognized in the literature (e.g.,). In fact, a precise knowledge of the axial gas dispersion coefficient is especially relevant for a reliable bubble column reactor design in case of liquid-gas reaction with high conversion of the gas phase [5]. Döß et al. [6] comprehensively summarized previous experimental and theoretical work on the topic, showing that the values of the axial gas dispersion coefficient can range between 0.001 and 1 m^2s^{-1} in the homogeneous regime, depending on column diameter, gas superficial velocity and physical properties of the fluids.

The conventional approach for determining axial dispersion coefficients relies on residence time measurements of a tracer injected at non-steady state conditions (e.g., as pulse or step) or injected at several axial positions at steady-state conditions. Since gas sampling at different axial positions is technically challenging, the first approach is preferred for gas dispersion measurements in bubble columns [1]. The use of tracers involves several drawbacks. Not only could the properties and, thus, the fluid dynamic behaviour of the system be altered, but also impurities or process downtime could detrimentally affect the system operations. Thus, Hampel [7] developed a non-invasive approach for determining the gas axial dispersion coefficient. In this approach, no tracer substance is needed, while a controlled marginal sinusoidal disturbance on the gas inlet flow is used as a virtual tracer instead. Accordingly, this modulation introduces a sinusoidal variation of the gas holdup in time, called gas holdup wave. Assuming that the gas holdup can be described using a one-dimensional axial dispersion model, the author has derived

$$\frac{\delta\epsilon}{\delta t} = D_{\mathrm{G}} \frac{\delta^2\epsilon}{\delta x^2} - u_{\mathrm{G}}^{*} \frac{\delta\epsilon}{\delta x}, \qquad 2$$

in analogy to Equation 1, where x is the axial position, ϵ is the gas holdup, that is a function of time and axial position, D_{G} is the axial gas dispersion coefficient and u_{G}^{*} is the bubble rise velocity. It should be noted that the use of a one-dimensional axial dispersion model requires the assumption

that the gas holdup is uniformly distributed in the column's cross-section. This assumption is fairly accepted in the homogeneous regime, as reported by Heijnen and Van't Riet [8]. Furthermore, the results reported by Kumar et al. [9] showed that a uniform distribution of the holdup in the homogeneous regime can be obtained with standard perforated plate spargers.

Along the column, the gas holdup wave is damped in amplitude (A_ϵ) and is shifted in phase (ϕ) due to the gas dispersion. Considering two different axial positions in the column, Hampel [7] related amplitude damping (V) and phase-shift ($\Delta\phi$) of the gas holdup wave to the axial dispersion coefficient as

$$V = \frac{A_\epsilon\,(x_2)}{A_\epsilon(x_1)} = \exp\left(\frac{u_\mathrm{G}^*}{2D_\mathrm{G}}\left[1 - \frac{1}{\sqrt{2}}\sqrt{1+\sqrt{1+\frac{16\omega^2 D_\mathrm{G}^2}{u_\mathrm{G}^{*\,4}}}}\right]\Delta x\right), \tag{3}$$

$$\Delta\phi = \phi(x_1) - \phi(x_2) = -\frac{u_\mathrm{G}^*}{D_\mathrm{G}\sqrt{8}}\left[\sqrt{\left[\sqrt{1+\frac{16\omega^2 D_\mathrm{G}^2}{u_\mathrm{G}^{*\,4}}}\right]-1}\right]\Delta x\,, \tag{4}$$

where Δx is the axial distance between the measuring points and ω is the angular modulation frequency. The evaluation of both V and $\Delta\phi$ between two axial positions requires measuring the time response of the gas density at two axial positions. A simplified scheme of the working principle of gas flow modulation is shown in **Figure 1**, together with the main elements of the experimental setup. It should be noted that a technique for measuring the gas holdup wave is also needed, although not included in **Figure 1**. A more detailed assessment of the experimental setup if gamma-ray densitometry is applied as measurement technique is available in Döß et al. [6].

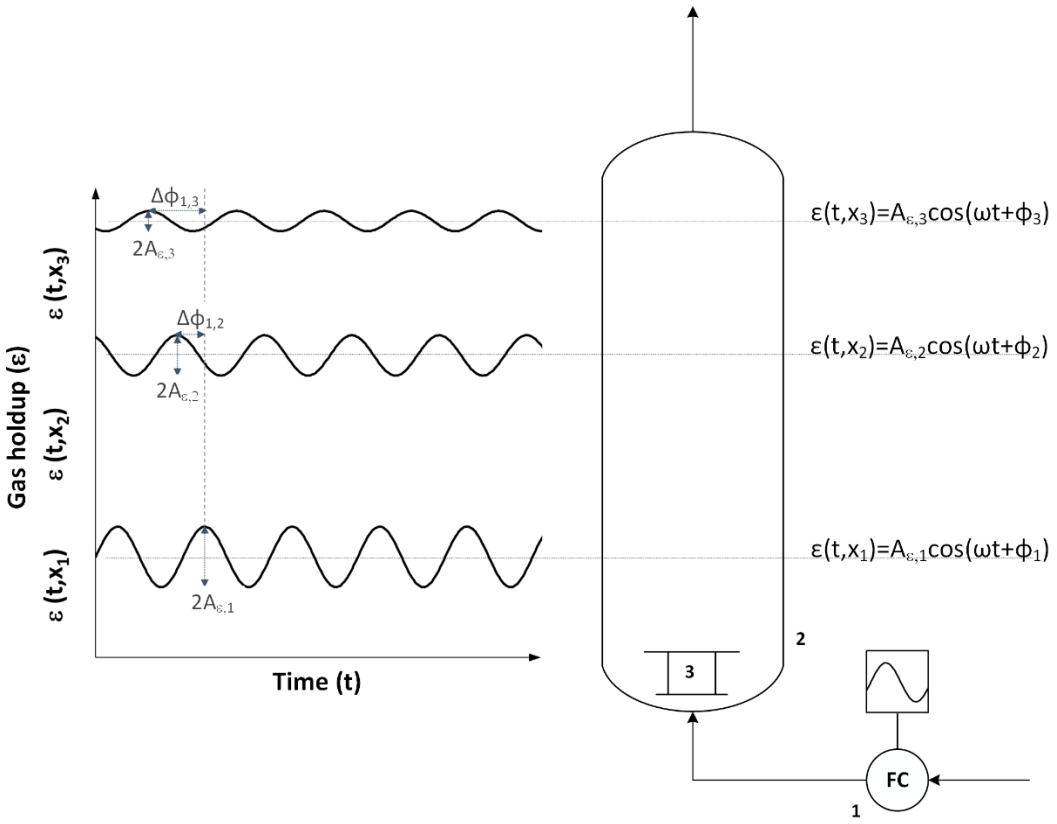

Figure 1. Simplified scheme of the gas flow modulation technique (1-gas flow modulator, 2-bubble column, 3-gas sparger).

Although the feasibility of the approach has already been shown [6], some open questions still need to be addressed, requiring further investigation.

Equation 1 was conceived to describe the concentration of a tracer substance in the considered phase as a function of space and time, where possible variations in the two-phase density are regarded as negligible side-effects. Instead, the gas flow modulation is based on a measurable change in the two-phase density, which might affect several characteristics of the bubble column, too, such as the bubble size and, thus, the bubble rise velocity. Therefore, whether Equation *2* (derived in analogy to Equation 1) is suitable or not to describe the gas holdup wave needs clarification. To evaluate the reliability of the obtained results, a quantification of the inherent uncertainties using Equation 2 and an analysis of the existence of multiple solutions for Equations 3 and 4 are also required. Furthermore, criteria for choosing optimal gas modulation parameters (i.e., modulation amplitude and modulation frequency) are still missing.

To address these objectives, this work provides a formal derivation of Equation 2, analyzes the assumptions that it implies and quantifies their impact on the obtained axial gas dispersion coefficient. Besides, the effects of the modulation parameters on the approach's sensitivity are evaluated together with the possibility of adapting them, based on the expected order of magnitude of the axial dispersion coefficient.

As mentioned above, Döß et al. [6] successfully applied sinusoidally-resolved gamma-ray densitometry to measure the gas holdup wave; other applicable measurement techniques are optical probes, pressure sensors and conductivity probes. However, it should be noted that this study provides a mathematical analysis that quantifies only the uncertainty directly related to the applied axial dispersion model, regardless of the applied measurement technique. The assessment of the experimental uncertainty is, instead, left for future work.

2. Derivation of the axial dispersion model applied to the gas holdup wave

This section reports the derivation of Equation 2 pointing out the assumptions that it implies. Referring to **Figure 2** and assuming that the mass-transfer between gas and liquid phase is negligible and source and sink terms are absent, the gas mass balance in the control volume (highlighted in red), of which the density is assumed constant, gives

$$\frac{\partial \epsilon}{\partial t} A \mathrm{d}x = u^*_{\mathrm{G,x}} A \epsilon_{\mathrm{x}} - u^*_{\mathrm{G,x+dx}} A \epsilon_{\mathrm{x+dx}} + J_{\mathrm{D,x+dx}} A - J_{\mathrm{D,x}} A \,, \qquad 5$$

where J_{D} is the dispersive volumetric flux referred to the entire column cross-sectional area (A). In reality, the gas density changes in the axial direction due to the hydrostatic pressure gradient. The implications of considering a constant gas density are assessed in the **Supplementary Information S1**.

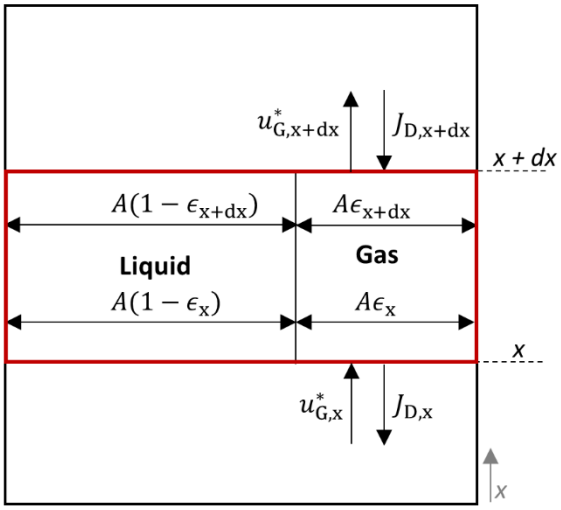

Figure 2. Scheme and nomenclature used in Equation 5.

Considering dispersion as a stochastic process that can be described using a diffusion-like law, the flux can be written as

$$J_{D,x} = D_G \frac{\partial \epsilon}{\partial x}, \qquad 6$$

whose orientation is opposite to the x-axis, as shown in **Figure 2**.

Equation 6 assumes that the axial dispersion coefficient is constant between the two measurement points. It should be noted that the dispersion flux J_D in Equation 5 is multiplied by the total cross-section of the column (A) and not by the section occupied by the gas ($A\epsilon$). This can be justified considering that in Equation 6 both the gas holdup and the axial gas dispersion coefficient are referred to the total column cross-section. Substituting Equation 6 in Equation 5 and assuming that the functions can be linearized in the interval of interest gives

$$\frac{\partial \epsilon}{\partial t} dx = u^*_{G,x}\epsilon_x - \left(u^*_{G,x}\epsilon_x + \frac{\partial u^*_G \epsilon}{\partial x} dx\right) - D_G \frac{\partial \epsilon}{\partial x}\Big|_x + \left(D_G \frac{\partial \epsilon}{\partial x}\Big|_x + D_G \frac{\partial^2 \epsilon}{\partial x^2} dx\right), \qquad 7$$

$$\frac{\partial \epsilon}{\partial t} dx = -\frac{\partial u^*_G \epsilon}{\partial x} dx + D_G \frac{\partial^2 \epsilon}{\partial x^2} dx, \qquad 8$$

$$\frac{\partial \epsilon}{\partial t} = -\epsilon \frac{\partial u^*_G}{\partial x} - u^*_G \frac{\partial \epsilon}{\partial x} + D_G \frac{\partial^2 \epsilon}{\partial x^2}. \qquad 9$$

The use of Equation 2 instead of Equation 9 can be justified if the bubble rise velocity is constant along the axis.

Provided that the measurements are performed at sufficient distance from the sparger, it can be assumed that the bubbles rise at their terminal velocity, which depends mainly on the gas and liquid physical properties and on the bubble size. Accordingly, constant bubble diameter applies between the measuring points. As a consequence, Equation 2 holds only for systems with negligible coalescence and breakup, and thus, can only be applied in case of the homogeneous regime. Another important implication is that the size of the bubbles detaching from the sparger is assumed constant over the entire modulation period. In other words, the change in the gas superficial velocity caused by the modulation brings a change in the number of bubbles only, but not in their size.

Furthermore, in a real system, the bubble size is expected to change due to the change in the gas density between the measurement points. This also causes a change in the bubble rise velocity. Its impact is quantified in the **Supplementary Information S2**.

Besides, the use of a one-dimensional axial dispersion model neglects all radial variations of gas holdup and bubble rise velocity. This hypothesis can also only be justified in case of the homogeneous regime, where gas holdup and bubble rise velocity are rather uniformly distributed as shown in the previous literature (e.g., [9]).

3. Uncertainty analysis

As analysed in the previous section, the use of Equation *2* implies the assumptions of constant bubble rise velocity and axial gas dispersion coefficient. This section aims at quantifying the impact of those assumptions on the obtained results.

3.1 Effect of a non-constant bubble rise velocity

The detachment of bubbles from orifices submerged in liquid has been extensively studied (e.g., [10-12]). Each orifice of the sparger is subsequently treated as a single capillary, where the bubbles are formed at pseudo-steady state (i.e., the formation time of the bubble is small compared to the modulation period). During the detachment process, the bubble is subjected to buoyancy, gas momentum, pressure difference between inside and outside the bubble, drag, inertia and surface tension. The gas momentum can be neglected considering that $\rho_G \ll \rho_L$. The pressure difference can be neglected if the inlet gas pressure is the same as the one of the bulk liquid at the same hydrostatic level. The force balance reported by Snabre and Magnifotcham [11], from which the bubble detachment diameter (d_B) can be derived, is

$$\frac{\pi}{3} d_B^3 \rho_L g = \left(\frac{81}{16} C_D + 9\alpha\right) \frac{\rho_L Q^2}{\pi d_B^2} + \pi d_h \sigma \,, \qquad 10$$

where Q is the gas flow rate exiting from each orifice of the sparger, C_D is the drag coefficient, α is the dimensionless inertial parameter, d_h is the orifice diameter and σ is the surface tension. The contribution of the surface tension is significant only at very low gas flow rates [12] and remains constant regardless of the gas flow rate changes. Since this study aims at quantifying the change in the bubble diameter with respect to the change in the gas flow rate, the contribution of the surface tension is left out, obtaining

$$d_B = \sqrt[5]{\frac{3}{\pi^2 g}\left(\frac{81}{16} C_D + 9\alpha\right) Q^2} \,. \qquad 11$$

Snabre and Magnifotcham [11] proposed that α can be assumed equal to $11/16$ and the drag coefficient can be estimated as

$$C_D = \frac{24}{Re} + 1 \,. \qquad 12$$

According to Equation 12, C_D depends on the gas flow rate. On the other hand, as shown by Snabre and Magnifotcham [11], an error of 10% in determining the drag coefficient leads to an error of less than 1% on the bubble diameter. In case of the gas flow modulation, a drag coefficient calculated using the average gas flow rate is considered fairly valid for the entire modulation

period. This is true especially for low-viscosity liquids at intermediate gas flow rates when $Re \gg 30$ and $C_D \approx 1$. Assuming $C_D = \text{const}$, the bubble diameter can be expressed as a function of the gas flow rate as

$$d_B = \sqrt[5]{\frac{3}{\pi^2 g}\left(\frac{81}{16}\bar{C}_D + 9\alpha\right)} Q^{\frac{2}{5}} \equiv H(\overline{Re})Q^{\frac{2}{5}}. \quad 13$$

For easier mathematical treatment, the dimensionless variable

$$\hat{d}_B = \frac{d_B}{\bar{d}_B} \quad 14$$

can be defined, referred to as fractional variation, where $\bar{d}_B$ and d_B are the average and the instant value of the bubble detachment diameter, respectively. Accordingly, Equation 13 can be written as

$$\hat{d}_B = \frac{1}{\bar{d}_B} H(\overline{Re})Q^{\frac{2}{5}} = \hat{Q}^{\frac{2}{5}}. \quad 15$$

Further, it can also be shown that $\hat{Q} = \hat{u}_G$ since

$$\hat{Q} = \frac{Q}{\bar{Q}} = \frac{n_f Q}{A} \cdot \frac{A}{n_f \bar{Q}} = \frac{u_G}{\bar{u}_G} = \hat{u}_G, \quad 16$$

where n_f is the total number of sparger holes and u_G is the gas superficial velocity.

Substituting Equation 16 in Equation 15 gives

$$\hat{d}_B = \hat{u}_G^{\frac{2}{5}}. \quad 17$$

The bubble rise velocity in columns of liquid has also been extensively studied and several models and correlation have been suggested. The bubble rise velocity has been described by Haberman and Morton [13] as a function of the bubble diameter as

$$u_G^* = \frac{1.02}{\sqrt{2}}\sqrt{g d_B}. \quad 18$$

Although this correlation is applicable only in certain ranges of fluid viscosity, density and surface tension and does not properly take into account the influence of the fluid properties on the bubble rise velocity, it can be considered fairly acceptable for a wide range of fluids used in the chemical industry [13]. In this study, it is preferred over more accurate correlations, because of its simple formulation.

In terms of the fractional variation, Equation 18 can be rewritten using Equation 17 as

$$\hat{u}_{\mathrm{G}}^{*} = \sqrt{\hat{d}_{\mathrm{B}}} = \sqrt[5]{\hat{u}_{\mathrm{G}}}\,. \tag{19}$$

Several correlations have been developed to express the gas holdup as a function of the gas superficial velocity. In case of air-liquid systems Hikita and Kikukawa [14] proposed

$$\epsilon = 0.505\, u_{\mathrm{G}}^{0.47} \left(\frac{0.072}{\sigma}\right)^{\frac{2}{3}} \left(\frac{0.001}{\mu_{\mathrm{L}}}\right)^{0.05}, \tag{20}$$

that, in terms of the fractional variation, becomes

$$\hat{\epsilon} = \hat{u}_{\mathrm{G}}^{0.47}. \tag{21}$$

Combining Equations 19 and 21, the fractional variation of the bubble rise velocity can be expressed as a function of the fractional variation of the gas holdup as

$$\hat{u}_{\mathrm{G}}^{*} = \hat{\epsilon}^{0.43}, \tag{22}$$

which leads to

$$\frac{\delta \hat{u}_{\mathrm{G}}^{*}}{\delta \hat{\epsilon}} = 0.43\, \hat{\epsilon}^{-0.57}\,. \tag{23}$$

The ratio between the second and third term of Equation 9 is, therefore, given by

$$\frac{-\epsilon \dfrac{\partial u_{\mathrm{G}}^{*}}{\partial x}}{-u_{\mathrm{G}}^{*} \dfrac{\partial \epsilon}{\partial x}} = \frac{\hat{\epsilon}}{\hat{u}_{\mathrm{G}}^{*}} \frac{\partial \hat{u}_{\mathrm{G}}^{*}}{\partial \hat{\epsilon}} = 0.43 \frac{\hat{\epsilon}^{-0.57} \hat{\epsilon}}{\hat{\epsilon}^{0.43}} = 0.43. \tag{24}$$

The value of this ratio shows that the two terms are of the same order of magnitude and neither of them is negligible. It should be noted that the exact value of the ratio depends on the selection of the respective correlations, which are used to relate gas holdup and bubble rise velocity to the gas superficial velocity, however, it can be taken as fairly representative for a qualitative analysis.

Using Equation 24, the second and third terms of Equation 9, can be written as

$$-\left(\epsilon\frac{\partial u_{\mathrm{G}}^{*}}{\partial x}+u_{\mathrm{G}}^{*}\frac{\partial \epsilon}{\partial x}\right)=-1.43\,u_{\mathrm{G}}^{*}\frac{\partial \epsilon}{\partial x}\,. \tag{25}$$

Accordingly, Equation 9 becomes

$$\frac{\partial \epsilon}{\partial t}=-1.43\,u_{\mathrm{G}}^{*}\frac{\partial \epsilon}{\partial x}+D_{\mathrm{G}}\frac{\partial^{2}\epsilon}{\partial x^{2}}\,. \tag{26}$$

Substituting Equation 22 in Equation 26 leads to

$$\frac{\partial \epsilon}{\partial t}=-1.43\frac{\bar{u}_{\mathrm{G}}^{*}}{\bar{\epsilon}^{0.43}}\epsilon^{0.43}\frac{\partial \epsilon}{\partial x}+D_{\mathrm{G}}\frac{\partial^{2}\epsilon}{\partial x^{2}}\,. \tag{27}$$

This equation requires the following initial and boundary conditions:

$$\epsilon(t)|_{\mathrm{x}=0}=\bar{\epsilon}\left[1+A_{\epsilon,0}\cos(\omega t+\phi)\right], \tag{28}$$

$$\epsilon(t)|_{\mathrm{x}\to\infty}=\bar{\epsilon}\,, \tag{29}$$

$$\epsilon(x)|_{\mathrm{t}=0}=\bar{\epsilon}\,, \tag{30}$$

where $A_{\epsilon,0}$ is the initial modulation amplitude. The time needed to reach quasi steady-state is discarded for a fair comparison.

It should be noted that Equation 25 is only valid above the sparger region if the bubbles rise with the same velocity as those at the sparger described by the local value of ϵ. This assumption is clearly a simplification, however, it is still maintained for the purpose of this qualitative study.

Equation 27 was solved numerically to describe the variation of the gas holdup in time at selected axial positions. The results were fitted using the function

$$\epsilon = \bar{\epsilon}[1 + A_{\epsilon}\cos(\omega t + \phi)]\,. \qquad 31$$

For the comparison of the results obtained from Equations 2 and 27, the deviations are defined as

$$\mathrm{Dev}V \quad = \frac{\mathrm{V(Eq.\,27)} - \mathrm{V(Eq.\,2)}}{\mathrm{V(Eq.\,27)}}, \qquad 32$$

$$\mathrm{Dev}\Delta\phi \quad = \frac{\Delta\phi\mathrm{(Eq.\,27)} - \Delta\phi\mathrm{(Eq.\,2)}}{\Delta\phi\mathrm{(Eq.\,27)}}. \qquad 33$$

For given values of bubble rise velocity and average holdup, the differences in amplitude damping and phase-shift predicted by Equations 2 and 27, respectively, were evaluated at different axial distances between the measurement points (**Figures 3a** and **3b**) and for various modulation frequencies (**Figures 3c** and **3d**) as a function of the axial gas dispersion coefficient.

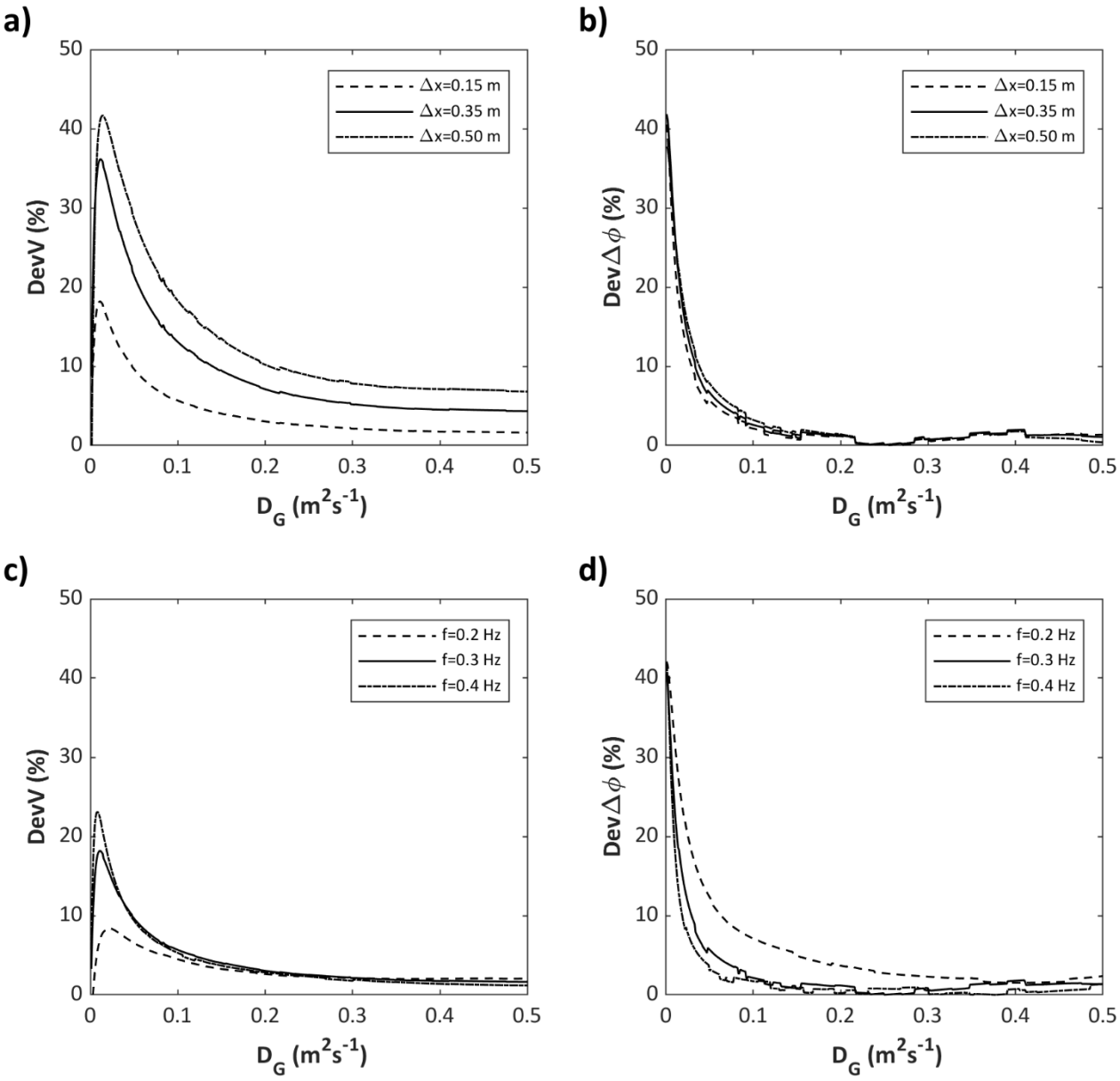

Figure 3. Deviations in amplitude damping and phase-shift caused by the use of Equation 2 for given values of average gas holdup and bubble rise velocity ($\bar{\epsilon} = 0.1$; $\bar{u}_G^* = 0.2$ ms^{-1}) as a function of the axial gas dispersion coefficient D_G for different axial distances between measuring points Δx (modulation frequency f = 0.3 Hz) (a, b) and for different modulation frequencies f (axial distance Δx = 0.15 m) (c, d).

Other examples of the same assessment, given different average values of bubble rise velocity and gas holdup, are reported in the **Supplementary Information S3**. As shown in **Figure 3**, the impact that the assumed constant bubble rise velocity on predicted amplitude damping and

phase-shift is higher for low values of the axial gas dispersion coefficient ($D_G < 0.1\ m^2s^{-1}$), while it tends to zero as the axial gas dispersion coefficient increases. The magnitude of the axial dispersion coefficient strongly depends on bubble rise velocity and column diameter, as shown by the correlations available in the literature (e.g., [15]). However, a range of 0.01-1 m^2s^{-1} can be considered representative for columns up to 1 m diameter operating in the homogeneous regime with water as working fluid. Higher values can be found in case of bigger columns or more viscous fluids. Thus, the use of Equation 2 can be justified regardless of the selected axial distance or modulation frequency for $D_G > 0.1\ m^2s^{-1}$, that fairly covers the range mentioned above. However, when low values of the axial gas dispersion coefficient are expected, reducing modulation frequency and axial distance can lower the uncertainty. On the other hand, it should be noted that for low values of the axial gas dispersion coefficient, the sensitivity is higher (see Section 4.1) and the deviation in the amplitude damping has, thus, less impact in that region.

3.2 Effect of a non-constant gas dispersion coefficient

As already mentioned in Section 2, the use of Equation 2 assumes that the axial dispersion coefficient is constant over the entire modulation period and between the selected measuring positions. The axial dispersion coefficient is commonly described by empirical correlations considering column diameter, gas superficial velocity and bubble rise velocity [6]. Among others, Mangartz and Pilhofer [15] proposed

$$D_G = 50 d_C^{1.5} {u_G^*}^3 , \qquad 34$$

where d_C is the column diameter. The effect of the holdup modulation on the calculated value of the axial dispersion coefficient can be assessed in analogy to Section 3.1.

Defining the dimensionless variable $\widehat{D}_G$, as

$$\widehat{D}_G = \frac{D_G}{\overline{D}_G} \qquad 35$$

and using Equation 22, Equation 34 can be rewritten as

$$\widehat{D}_{\mathrm{G}} = \hat{\epsilon}^{1.29}\,. \qquad 36$$

Since the bubble rise velocity is related to the detachment conditions at the sparger, the dimensionless gas holdup is a function of the initial modulation amplitude according to

$$\hat{\epsilon} = \frac{\bar{\epsilon}\left[1 + A_{\epsilon,0}\cos(\omega t + \phi)\right]}{\bar{\epsilon}}\,. \qquad 37$$

The value of $\hat{\epsilon}$ varies between an upper and lower limit as

$$\hat{\epsilon}_{\min} = 1 - A_{\epsilon,0} < \hat{\epsilon} < 1 + A_{\epsilon,0} = \hat{\epsilon}_{\max}\,. \qquad 38$$

Accordingly, the value of $\widehat{D}_{\mathrm{G}}$ also oscillates between a lower and upper limit during the modulation period corresponding to $\hat{\epsilon}_{\min}$ and $\hat{\epsilon}_{\max}$, respectively. The variation of D_{G} from the average value can be defined as a function of $\hat{\epsilon}$, considering Equation 36, as

$$\mathrm{Dev}D_{\mathrm{G}} = \frac{D_{\mathrm{G}} - \overline{D}_{\mathrm{G}}}{\overline{D}_{\mathrm{G}}} = \widehat{D}_{\mathrm{G}} - 1 = \hat{\epsilon}^{1.29} - 1\,. \qquad 39$$

The upper and lower limits of $\mathrm{Dev}D_{\mathrm{G}}$ within the modulation period can be determined considering Equation 38 as

$$\mathrm{Dev}D_{\mathrm{G,min}} = (1 - A_{\epsilon,0})^{1.29} - 1 < \mathrm{Dev}D_{\mathrm{G}} < (1 + A_{\epsilon,0})^{1.29} - 1 = \mathrm{Dev}D_{\mathrm{G,max}}. \qquad 40$$

Equation 40 shows that maximum and minimum of $\mathrm{Dev}D_{\mathrm{G}}$ in the modulation period only depend on the initial modulation amplitude (see also **Figure 4**) and not on the modulation frequency.

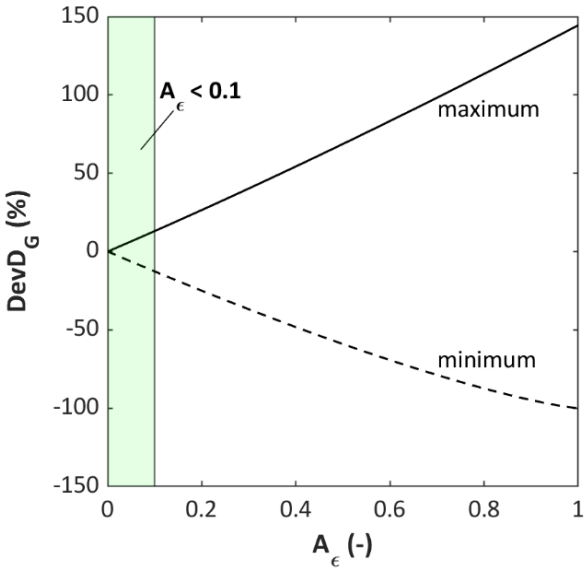

Figure 4. Lower and upper limit of the variation of the axial gas dispersion coefficient as a function of the initial modulation amplitude A_ϵ. The green area highlights the recommended range of values of the initial modulation amplitude to be used during experiments.

Döß et al. [6] performed an uncertainty analysis for two cases, using the correlation of Bach and Pilhofer [16] (relating holdup and gas superficial velocity) and Mangartz and Pilhofer [15] (relating axial dispersion coefficient and bubble rise velocity) and assuming the bubble rise velocity as

$$u_{\mathrm{G}}^{*} = \frac{u_{\mathrm{G}}}{\epsilon}. \qquad 41$$

The dependence of Dev$D_{\mathrm{G,min}}$ and Dev$D_{\mathrm{G,max}}$ only from the modulation amplitude (see **Figure 4**) can also be found in the data reported by Döß et al. [6], although their uncertainty is higher than the one obtained here, which can be attributed to the selection of different correlations. It should also be mentioned that the uncertainty shown in **Figure 4** is an overestimation of the real uncertainty. In fact, although the local conditions oscillate between the corresponding values of minimum and maximum modulation, the presented analysis considers a column operating at the maximum or minimum of the modulation. However, we agree with the authors that the initial modulation amplitude ($A_{\epsilon,0}$, as shown in Equation 37) should be kept, if possible, below 0.1 to provide a more reliable determination of the axial dispersion coefficient.

3.3 Ambiguities caused by the existence of multiple solutions

This section aims at analyzing the ambiguities caused by the existence of multiple solutions while calculating D_G from Equations 3 and 4. **Figure 5** shows an example of the predicted amplitude damping and phase-shift at various axial positions as a function of the axial dispersion coefficient for given values of modulation amplitude and frequency and bubble rise velocity. Other examples are reported in the **Supplementary Information S4** for different values of f and u_G^*.

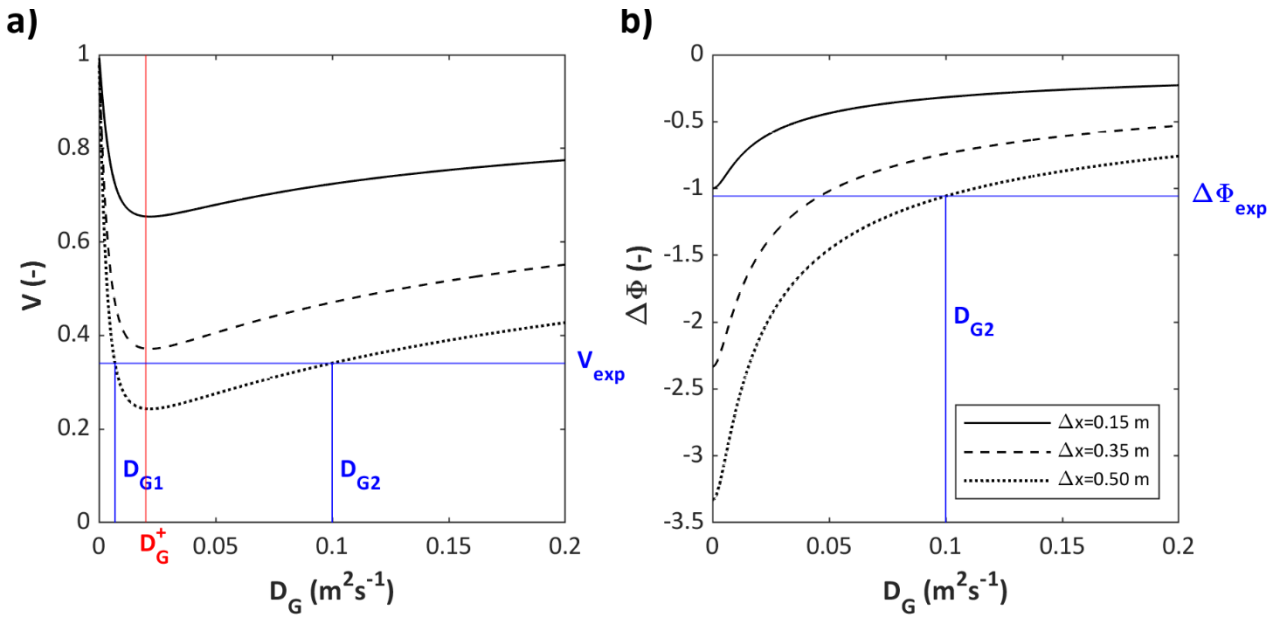

Figure 5. Predicted amplitude damping (a) and phase-shift (b) as a function of the axial dispersion coefficients considering f =0.3 Hz and u_G^* =0.2 m/s (D_{G1} and D_{G2} illustrate the existence of multiple solutions for a given set of measured amplitude damping and phase-shift).

Figure 5a shows that more than one solution can exist extracting D_G from Equation 3 for a given amplitude damping. Contrary, given a certain column geometry and operating conditions, the corresponding value of the axial gas dispersion coefficient is unique and can be uniquely determined when Equation 4 is considered (**Figure 5b**). **Figure 5a** also shows that the predicted amplitude damping has a minimum. The axial dispersion coefficient value that corresponds to the minimum amplitude damping will be referred to as D_G^+. The first derivative of Equation 3 can be analyzed to study the existence of the minimum and, thus, of multiple solutions.

The first derivative of the amplitude damping with respect to the axial gas dispersion coefficient is

$$\frac{dV}{dD_{\mathrm{G}}} = \left[-\frac{C_1}{D_{\mathrm{G}}^2} + \frac{C_1}{\sqrt{2}D_{\mathrm{G}}^2}\sqrt{1+\sqrt{1+C_2D_{\mathrm{G}}^2}} - \frac{C_1C_2}{2\sqrt{2}\sqrt{1+C_2D_{\mathrm{G}}^2}\sqrt{1+\sqrt{1+C_2D_{\mathrm{G}}^2}}} \right] \cdot$$

$$\cdot \exp\left(\frac{C_1}{D_G}\left[1 - \frac{1}{\sqrt{2}}\sqrt{1+\sqrt{1+C_2D_{\mathrm{G}}^2}} \right] \right) \qquad 42$$

where $C_1 = u_{\mathrm{G}}^* \, \Delta x/2$ and $C_2 = 16\omega^2/{u_{\mathrm{G}}^*}^4$. The value of D_{G}^+ can be determined solving

$$\frac{1}{D_{\mathrm{G}}^2}\left(1 - \frac{1}{\sqrt{2}}\sqrt{1+\sqrt{1+C_2D_{\mathrm{G}}^2}} \right) + \frac{C_2}{2\sqrt{2}\sqrt{1+C_2D_{\mathrm{G}}^2}\sqrt{1+\sqrt{1+C_2D_{\mathrm{G}}^2}}} = 0\,. \qquad 43$$

Defining

$$K = \sqrt{1+C_2D_{\mathrm{G}}^2}\,, \qquad 44$$

Equation 43 can be rewritten as

$$\frac{1}{K^2-1}\left(1 - \frac{1}{\sqrt{2}}\sqrt{1+K} \right) + \frac{1}{2\sqrt{2}K\sqrt{1+K}} = 0 \qquad 45$$

Equation 45 has only one real solution, given by $K = 2+\sqrt{5}$. Substituting this solution into Equation 44, D_{G}^+ can be obtained as

$$D_{\mathrm{G}}^+ = 2\sqrt{\frac{2+\sqrt{5}}{C_2}} = 2\sqrt{\frac{{u_{\mathrm{G}}^*}^4(2+\sqrt{5})}{16\omega^2}} = \frac{{u_{\mathrm{G}}^*}^2}{2\omega}\sqrt{2+\sqrt{5}}\,. \qquad 46$$

Equation 46 shows that the minimum of the amplitude damping always exists accompanied by two solutions of Equation 3 (at least in parts of the domain).

An analogous analysis can be done considering Equation 4, whose derivative with respect to D_{G} is

$$\frac{d\Delta\Phi}{dD_{\mathrm{G}}} = \frac{C_1}{\sqrt{2}D_{\mathrm{G}}^2}\sqrt{\sqrt{1+C_2D_{\mathrm{G}}^2}-1} - \frac{C_1C_2}{2\sqrt{2}\sqrt{C_2D_{\mathrm{G}}^2+1}\sqrt{\sqrt{C_2D_G^2+1}-1}}. \qquad 47$$

Stationary points in the function described by Equation 4 are given by the solution of

$$\frac{\sqrt{K-1}}{(K^2-1)} - \frac{1}{2K\sqrt{K-1}} = 0\,. \qquad 48$$

Considering that $C_2 > 0$ and, thus, $K > 0$, Equation 48 has no real solution. Therefore, Equation 4 has only one solution in terms of D_{G} for a given phase-shift. This means that the phase-shift corresponding to given column geometry, bubble rise velocity and modulation parameters is uniquely defined.

The value of D_{G} can be extracted from Equation 4 as

$$\mathrm{D_G} = \sqrt{\frac{C_1^4}{4\Delta\phi^4}\left(C_2 - \frac{4\Delta\phi^2}{C_1^2}\right)}. \qquad 49$$

As pointed out by Döß et al. [6], the condition required to avoid complex solutions in terms of D_G is

$$|\Delta\phi| < \frac{\omega\Delta x}{u_{\mathrm{G}}^*}. \qquad 50$$

However, substituting Equation 4 in Equation 50 gives

$$\frac{u_{\mathrm{G}}^*}{D_{\mathrm{G}}\sqrt{8}}\left[\sqrt{\left[\sqrt{1+\frac{16\omega^2D_{\mathrm{G}}^2}{{u_{\mathrm{G}}^*}^4}}\right]-1}\right]\Delta x < \frac{\omega\Delta x}{u_{\mathrm{G}}^*} \qquad 51$$

that leads to

$$\frac{64\omega^4 D_G^4}{u_G^{*\,8}} > 0\,. \qquad 52$$

Equation 52 and, thus, the condition expressed by Equation 50 are always valid. Accordingly, Equation 49 has always a real solution regardless of the operating parameters. However, considering a sinusoidal gas holdup wave, the phase at a certain axial position can only be determined with $\pm 2n\pi$, with n being a positive integer. To allow a reliable quantification of the phase-shift, it must be ensured that

$$|\Delta\phi| < 2\pi\,. \qquad 53$$

As shown in **Figure 5b**, $|\Delta\phi|$ increases monotonously with decreasing D_G, thus, Equation 53, can be written as

$$|\Delta\phi| < |\Delta\phi|_{D_G \to 0} < 2\pi\,. \qquad 54$$

Since

$$|\Delta\phi|_{D_G \to 0} < \frac{C_1\sqrt{C_2}}{2} = \frac{\Delta x\omega}{u_G^*}, \qquad 55$$

the condition

$$\frac{\Delta x\omega}{u_G^*} < 2\pi \qquad 56$$

guarantees that the value of the phase-shift is always lower than 2π for every value of the axial gas dispersion coefficient. If this condition is fulfilled, the gas dispersion coefficient is uniquely determined, assuming that the average bubble rise velocity is known.

3.4 Effect of the unknown bubble rise velocity

As shown in the previous section, once the bubble rise velocity is known, the axial gas dispersion coefficient can be uniquely determined. Döß et al. [6] proposed to estimate the bubble rise velocity as u_G/ϵ, which is also known as the bubble swarm velocity. However, this can only give a rough

estimate. The same holds for the correlations discussed in Section 3.1. The uncertainty of the bubble rise velocity introduces an uncertainty in the determined axial gas dispersion coefficient, too, which is analyzed in this section. Amplitude damping and phase-shift have been predicted using Equations 3 and 4 for given values of f, D_G, u_G^* and Δx. The predicted amplitude damping and phase-shift have been kept constant, while the effect of varying u_G^* ±20% on D_G was studied. The results of this analysis are shown in **Figure 6** considering

$$\mathrm{Err}D_G = \frac{D_{G,\mathrm{calculated}} - D_{G,\mathrm{real}}}{D_{G,\mathrm{real}}} \qquad 57$$

The influence of the modulation frequency was also analyzed and is reported in **Figure 6**. The uncertainty is independent of the axial distance between the measuring points, as shown in the **Supplementary Information S5**, where also other examples for different values of D_G and u_G^* are reported.

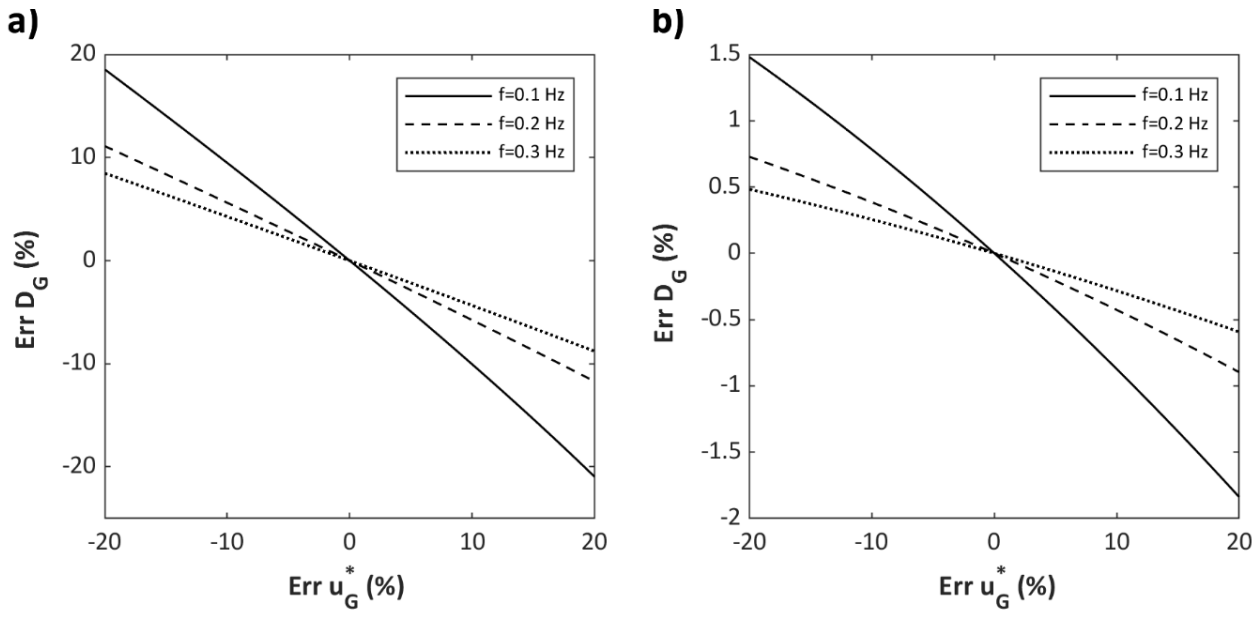

Figure 6. Error of the determined axial gas dispersion coefficient using Equation 3 (a) or 4 (b) introduced by an incorrect bubble rise velocity Err u_G^* for $D_G = 0.1\ \mathrm{m^2 s^{-1}}$, $u_G^* = 0.1\ \mathrm{ms^{-1}}$ and $\Delta x = 0.15$ m (non-physical solution of Equation 3 are not reported).

Figure 6 shows that an incorrect bubble rise velocity has a severe impact on the axial gas dispersion coefficient when Equation 3 (based on amplitude damping) is used, while it is

negligible for Equation 4 (based on phase-shift). Therefore, the axial dispersion coefficient determined using the phase-shift equation can be considered more reliable.

4. Sensitivity analysis

Ensuring an adequate sensitivity of amplitude damping and phase-shift is crucial for a reliable calculation of the axial gas dispersion coefficient. The sensitivity is represented by the first derivatives of both amplitude damping and phase-shift with respect to the axial gas dispersion coefficient, which are shown in Equations 42 and 47, respectively. Referring to these equations, the sensitivity is a function of modulation frequency, axial distance between the measuring points, bubble rise velocity and axial gas dispersion coefficient, while it is independent of the modulation amplitude. The bubble rise velocity and the axial gas dispersion coefficient are natural results of given operating conditions and column dimensions and, thus, cannot be adjusted towards higher sensitivity. The modulation frequency and the axial distance between the measuring points, instead, can be freely chosen when performing experiments. An example of optimization of these parameters can be found in a case study reported in **the Supplementary Information S7**.

4.1 Effect of axial gas dispersion coefficient and bubble rise velocity

As shown in Equations 42 and 47, the sensitivity of both amplitude damping and phase-shift is a function of axial gas dispersion coefficient and bubble rise velocity. This effect is reported in **Figure 7** for the derivatives of amplitude damping and phase-shift. Other examples for different values of f and Δx are reported in the **Supplementary Information S6**.

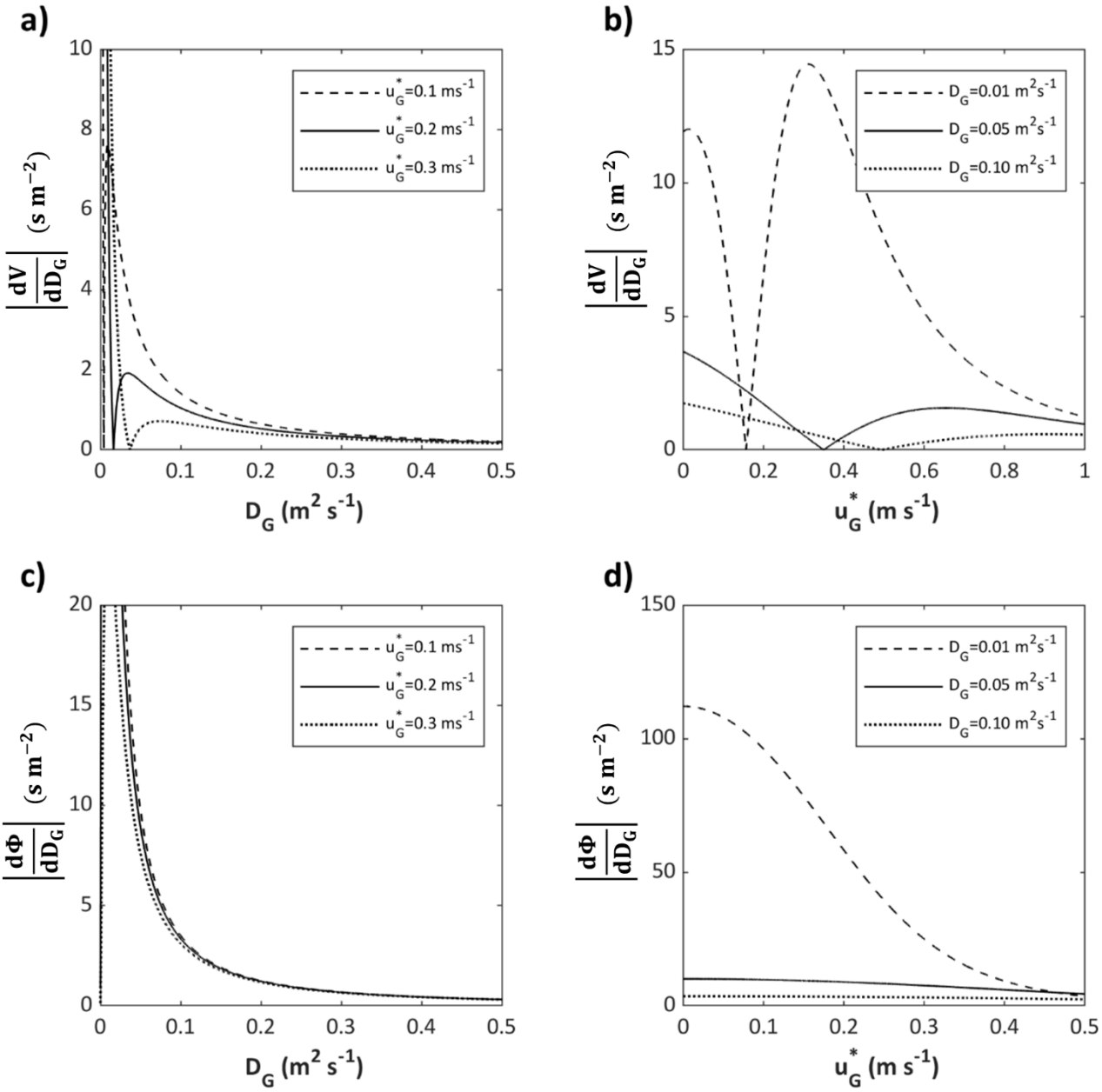

Figure 7. Sensitivity of the amplitude damping as a function of axial gas dispersion coefficient (a) and bubble rise velocity (b) and sensitivity of the phase-shift as a function of axial gas dispersion coefficient (c) and bubble rise velocity (d) for f = 0.4 Hz and Δx =0.2 m.

For both amplitude damping and phase-shift, low sensitivity coincides with higher values of axial gas dispersion coefficient and bubble rise velocity and vice versa. While the sensitivity of the phase-shift is never zero (for positive values of the axial gas dispersion coefficient), the amplitude damping always shows a point of zero sensitivity, corresponding to the condition (derived in Section 3.3)

$$\frac{u_G^{*\,2}}{2D_G\omega}\sqrt{2+\sqrt{5}}=1\,, \qquad 58$$

at which experiments must be avoided. Since bubble rise velocity and axial gas dispersion coefficient are a natural outcome of chosen operating conditions, column geometry and physical properties of the fluids, only the modulation frequency and the axial distance between the measurement points can be adjusted for this purpose as shown below.

4.2 Effect of the modulation frequency

Figure 8 shows the dependency of the sensitivity of the amplitude damping on the modulation frequency (according to Equation 42) for different values of bubble rise velocity and axial gas dispersion coefficient.

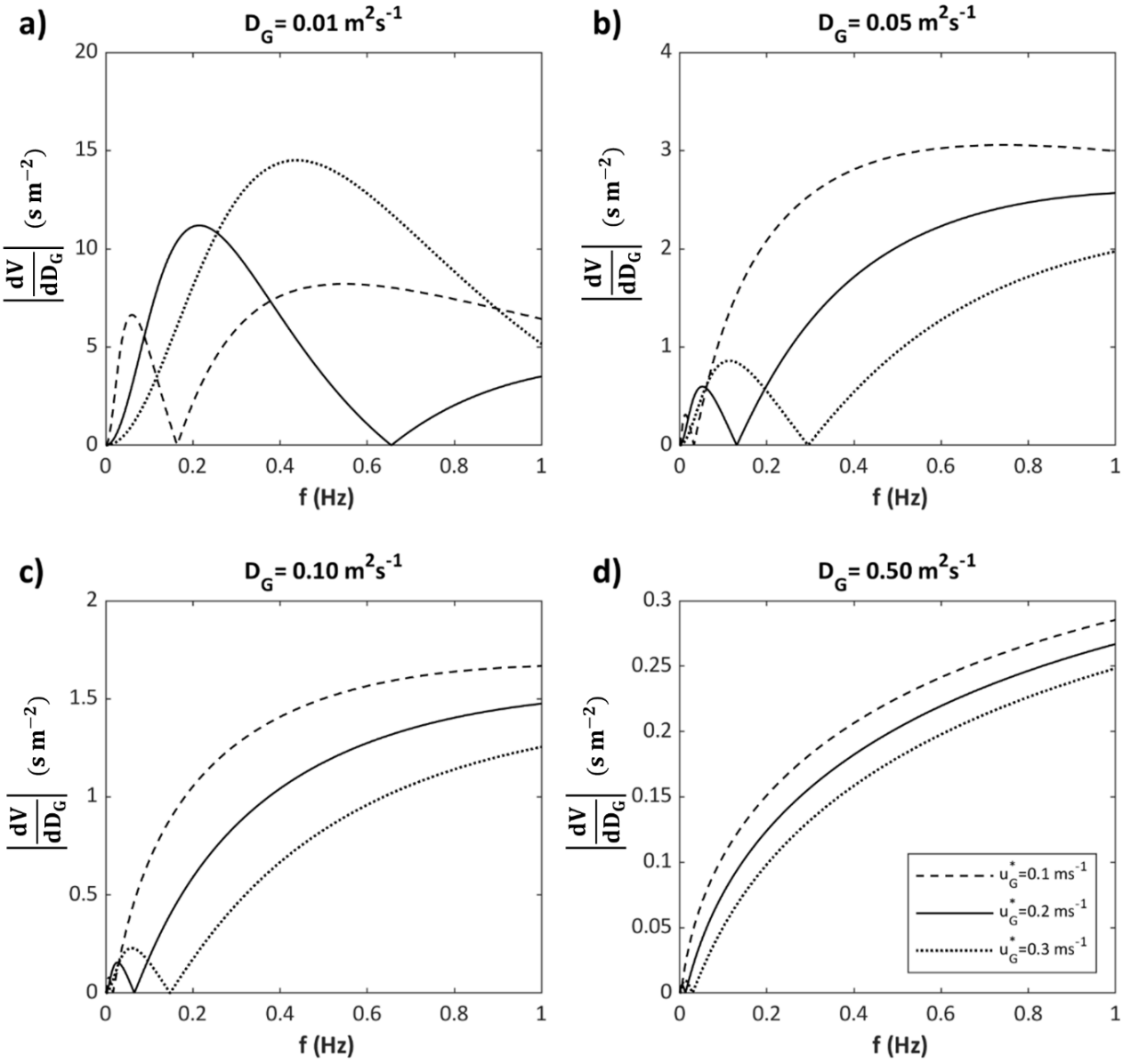

Figure 8. Sensitivity of the amplitude damping as a function of the modulation frequency for different bubble rise velocities and axial gas dispersion coefficients ($\Delta x = 0.2$).

The position of the point of zero sensitivity is again described by Equation 58. A change in the modulation frequency allows shifting this point far from the region of the expected value of the axial gas dispersion coefficient to ensure measurements with adequate sensitivity.

Figure 9 shows an example of how D_G^+ changes with the modulation frequency for given values of the bubble rise velocity.

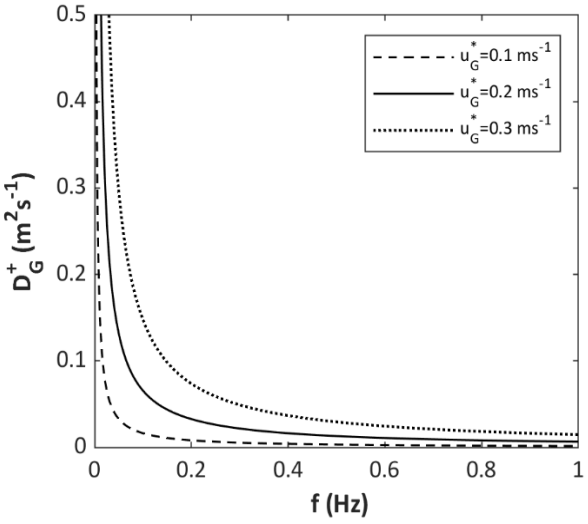

Figure 9. Axial dispersion coefficient corresponding to the minimum amplitude (D_G^+) as a function of the modulation frequency for given values of the bubble rise velocity.

Following Equation 46, **Figure 9** shows that D_G^+ can be shifted to higher values of the axial dispersion coefficient lowering the modulation frequency and vice versa. In this way, the modulation frequency can be selected to ensure that the expected axial gas dispersion coefficient is significantly higher or lower than D_G^+. The bubble rise velocity also affects the value of D_G^+, however, this parameter cannot be changed for given setup, fluids and operating conditions.

Figure 10 shows the dependency of the sensitivity of the phase-shift on the modulation frequency (according to Equation 47). The sensitivity increases with increasing modulation frequency regardless of the magnitude of bubble rise velocity and axial gas dispersion coefficient.

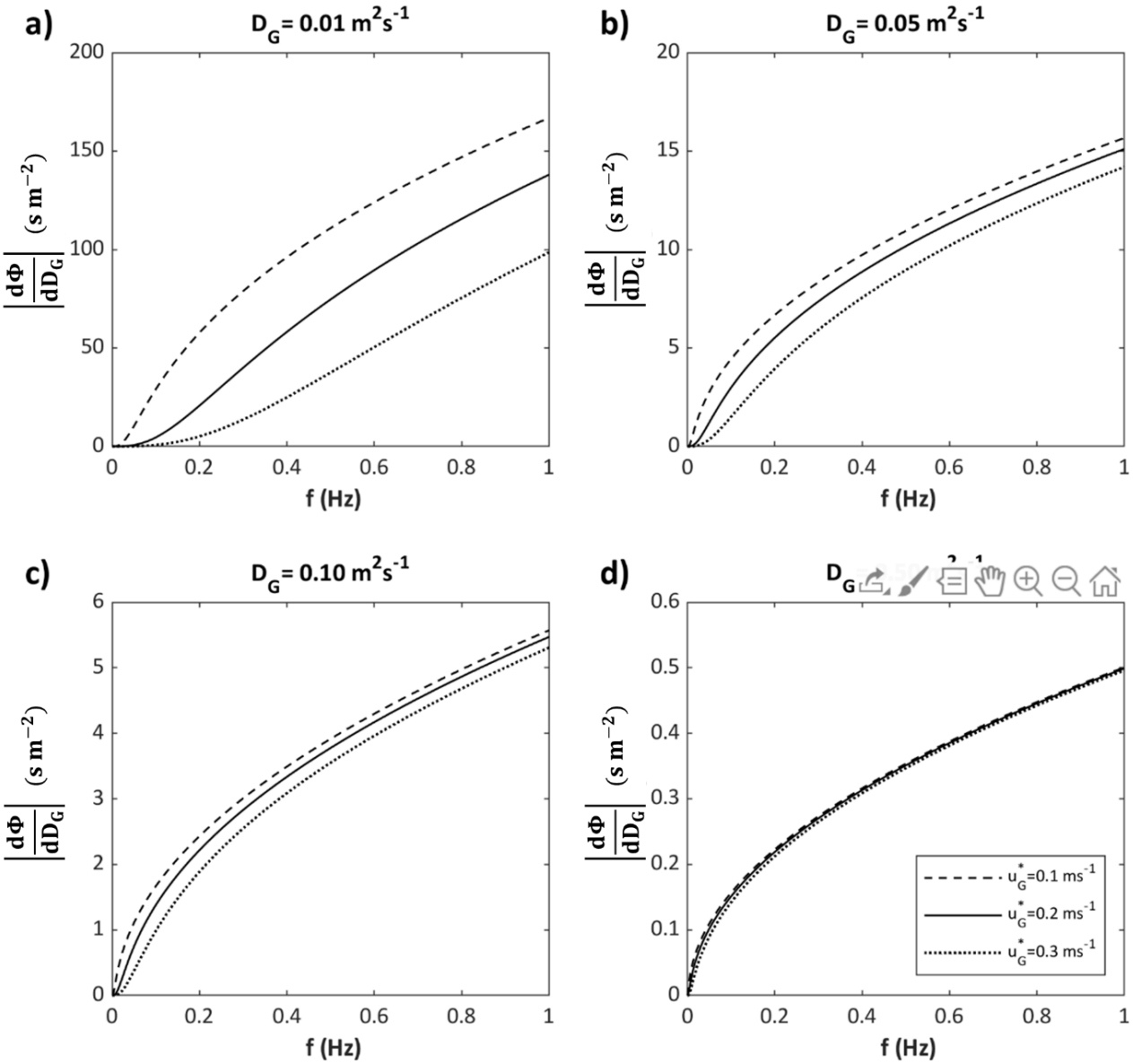

Figure 10. Sensitivity of the phase-shift as a function of the modulation frequency for different bubble rise velocities and axial gas dispersion coefficients ($\Delta x = 0.2$).

From the results reported in **Figures 8** and **10**, it can be concluded that modulation frequencies $\omega \gg \omega^+$, where

$$\omega^+ = \frac{u_G^{*\,2}}{2D_G}\sqrt{2+\sqrt{5}}\,, \qquad 59$$

are beneficial in terms of sensitivity. However, in case Equation 56 would be violated (e.g., for low values of D_G), $\omega \ll \omega^+$ should be satisfied instead.

4.3 Effect of the axial distance between measurement points

As analyzed in Section 3.3 the derivative of the amplitude damping depends on $C_1 = u_G^* \Delta x/2$ (refer to Equation 42), and, thus, on the axial distance between the measurement points. This effect is shown in **Figure 11** for different bubble rise velocities and axial gas dispersion coefficients.

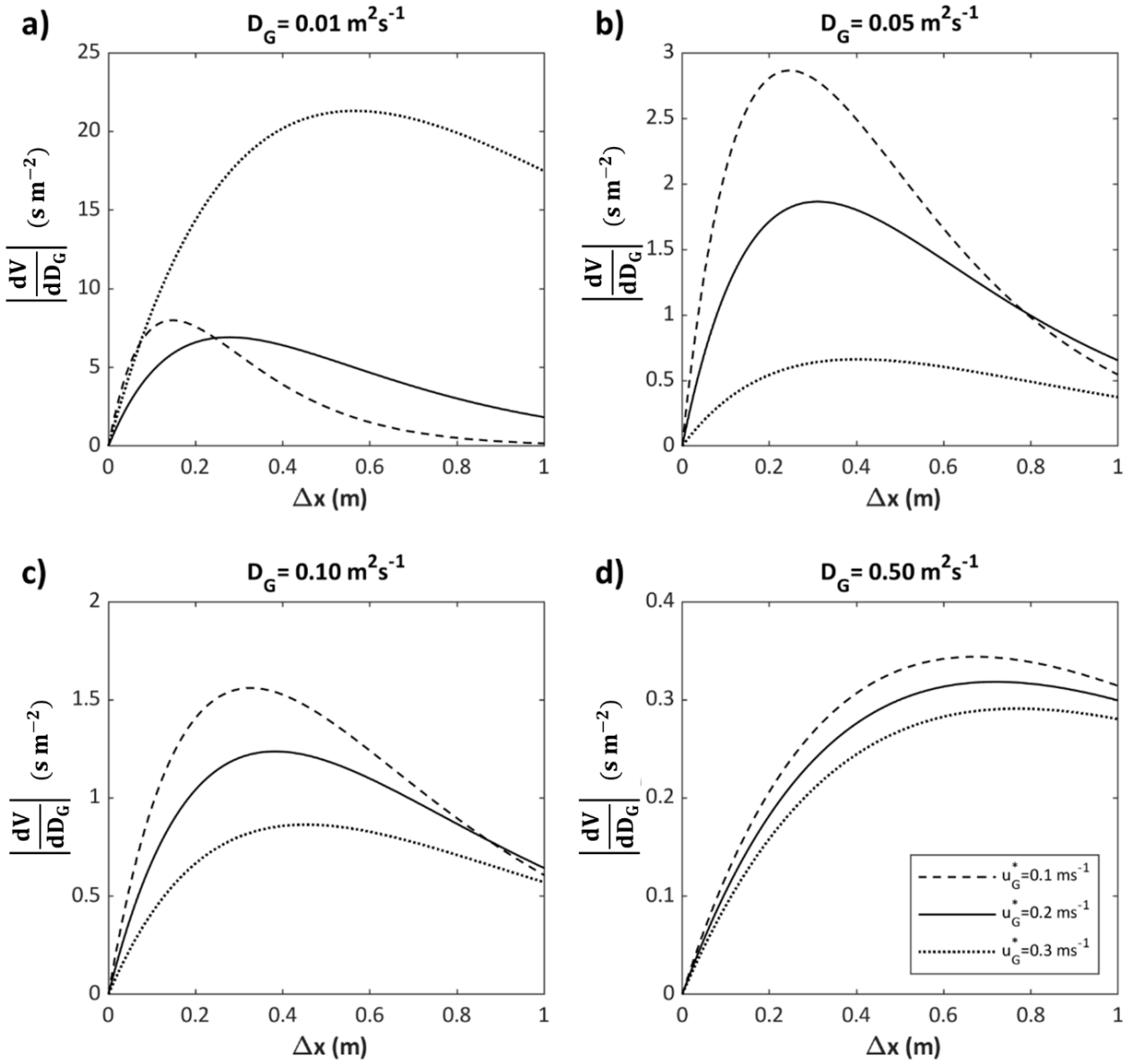

Figure 11. Sensitivity of the amplitude damping as a function of the axial distance between the measurement points for different bubble rise velocities and axial gas dispersion coefficients (f = 0.4 Hz).

The sensitivity shows a maximum corresponding to a certain axial distance value, referred to as Δx^+, that can be found analysing the derivative of the sensitivity with respect to the axial distance given by

$$\frac{d}{d\Delta x}\left(\frac{dV}{dD_{\mathrm{G}}}\right) = \frac{d}{d\Delta x}\left[\Delta x F_1 \exp(F_2 \Delta x)\right] = F_1 \exp(F_2 \Delta x) + \Delta x F_1 F_2 \exp(F_2 \Delta x)\,, \tag{60}$$

where

$$F_1 = \frac{u_{\mathrm{G}}^*}{2}\left[-\frac{1}{D_{\mathrm{G}}^2} + \frac{1}{\sqrt{2}D_{\mathrm{G}}^2}\sqrt{1+\sqrt{1+C_2 D_{\mathrm{G}}^2}} - \frac{C_2}{2\sqrt{2}\sqrt{1+C_2 D_{\mathrm{G}}^2}\sqrt{1+\sqrt{1+C_2 D_{\mathrm{G}}^2}}}\right], \tag{61}$$

$$F_2 = \frac{u_{\mathrm{G}}^*}{2D_G}\left[1 - \frac{1}{\sqrt{2}}\sqrt{1+\sqrt{1+C_2 D_{\mathrm{G}}^2}}\right]. \tag{62}$$

The stationary point of the function can be found solving

$$F_1 \exp(F_2 \Delta x) + \Delta x F_1 F_2 \exp(F_2 \Delta x) = 0 \tag{63}$$

that gives

$$\Delta x^+ = -\frac{1}{F_2}, \tag{64}$$

considering that F_2 has always negative values, Δx^+ always exists and its value depends on ω, D_{G} and u_{G}^*. Once the frequency has been chosen as reported in the previous section, the axial distance between the measuring points can be chosen close to Δx^+ based on the expected values of axial gas dispersion coefficient and bubble rise velocity. However, when selecting the axial distance, it should be considered that a higher Δx reduces the value of the amplitude on the upper point, increasing the experimental uncertainty related to that value.

In analogy, the influence of the axial distance on the sensitivity of the phase-shift has also been evaluated. Examples of the phase-shift sensitivity are reported in **Figure 12** for different bubble rise velocities and axial gas dispersion coefficients. The sensitivity of the phase-shift increases linearly with the axial distance (see also Equation 47).

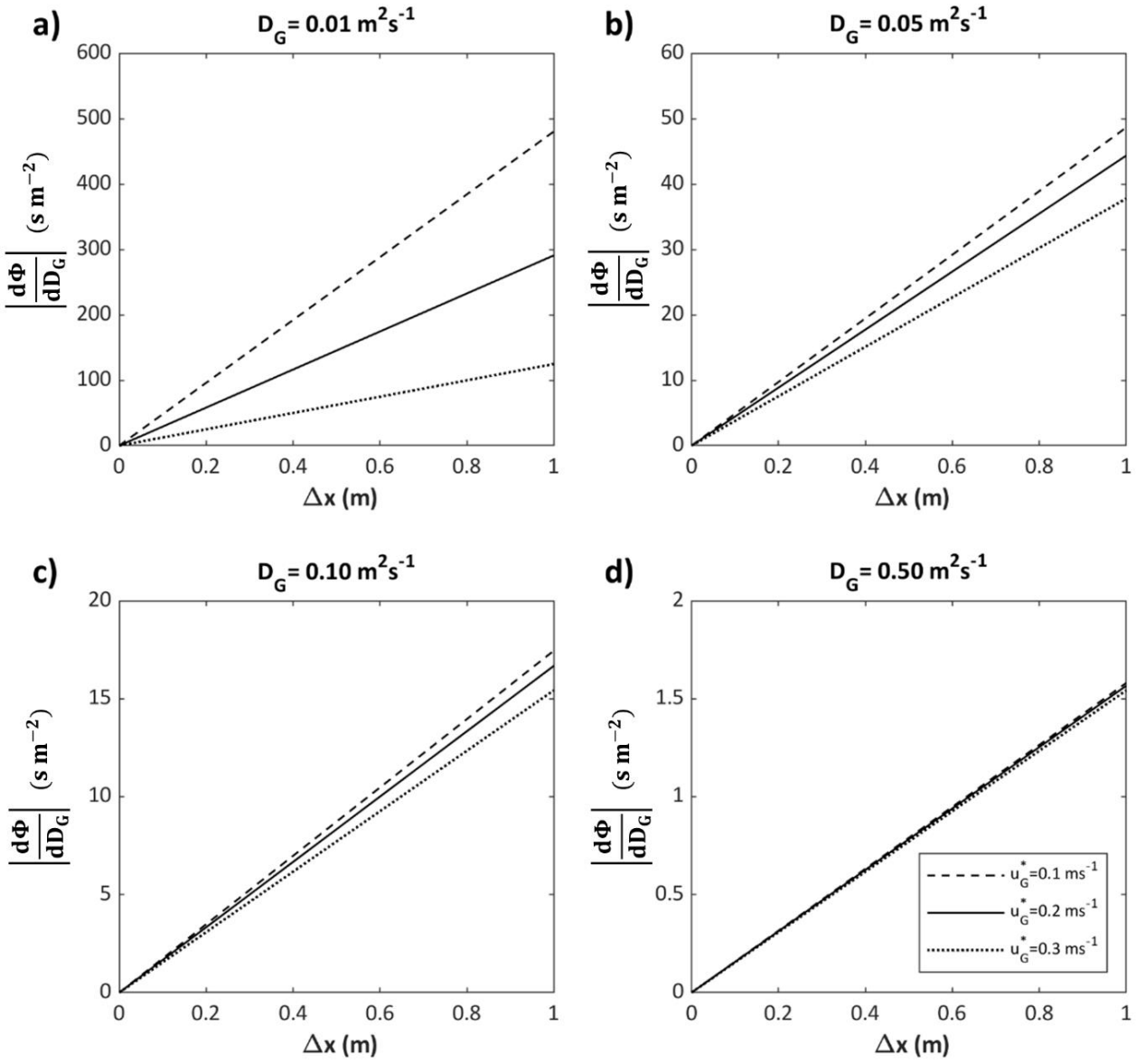

Figure 12. Sensitivity of the phase-shift as a function of the axial distance between the measurement points for different bubble rise velocities and axial gas dispersion coefficients.

5. Conclusions and future work

A formal derivation of the axial dispersion model equation applied to describe the gas holdup wave in time and space was presented. This allowed evaluating the effects of the assumptions involved, which are constant bubble rise velocity (that implies constant bubble size) and constant axial gas dispersion coefficient.

The impact of assuming a constant bubble rise velocity was assessed using established correlations available in the literature. The analysis showed a significant impact on the predicted amplitude damping and phase-shift only for very low values of the axial gas dispersion coefficient, where the sensitivity is also higher. The mentioned assumptions can, therefore, be considered fairly valid.

The assumption of constant axial gas dispersion coefficient causes uncertainty that increases with the initial modulation amplitude. It was shown that if the modulation amplitude is kept below 0.1, the maximum uncertainty is below ±20%. However, a low initial modulation amplitude also decreases the amplitude of the gas holdup wave at the measurement point, introducing experimental uncertainty. Quantification of this uncertainty was neglected in this work and will be addressed in the future.

The existence of a unique solution in terms of axial dispersion coefficient and the lower impact of uncertainty in the bubble rise velocity qualify the phase-shift as more reliable and self-sufficient for determining the axial gas dispersion coefficient. However, since the solution obtained using the phase-shift allows discarding the non-physical solution of the amplitude damping equation, the latter should also be considered to confirm the obtained results, especially in case of low sensitivity.

If values of bubble rise velocity and axial gas dispersion coefficient can be anticipated prior to the dispersion measurements (e.g., performing preliminary experiments, using correlations or data available in the literature), the analysis reported in this study allows selecting modulation frequency and axial distance between the measurement points that give the highest sensitivity.

In conclusion, this study confirms the gas flow modulation as a promising candidate for the experimental investigation of axial gas dispersion coefficients in bubble columns in the homogeneous flow regime.

However, the approach is unsuitable for measuring the axial gas dispersion coefficient in heterogeneous and transition bubble flow regimes, in which the coalescence and break up phenomena influence the bubble size. The development of an approach suitable for application in the heterogeneous regime is left for future work.

6. Acknowledgement

This work was supported by the German Research Foundation (DFG, HA 3088/18-1).

Nomenclature

Symbol	Description	Unit
A	Column cross-sectional area	m^2
A_ϵ	Amplitude of the gas holdup wave at the considered axial position	
$A_{\epsilon,0}$	Initial amplitude of the gas holdup wave	
c	Tracer concentration	$\mathrm{mol\ m}^{-3}$
C_1	Coefficient defined as $\frac{u_G^* \Delta x}{2}$	$\mathrm{m}^2\mathrm{s}^{-1}$
C_2	Coefficient defined as $\frac{16\omega^2}{{u_G^*}^4}$	$\mathrm{rad}^2\ \mathrm{m}^{-4}\mathrm{s}^2$
C_D	Drag coefficient	
$\bar{C}_\mathrm{D}$	Average drag coefficient	
d_B	Bubble diameter	m
$\bar{d}_\mathrm{B}$	Average bubble diameter	m
$\hat{d}_\mathrm{B}$	Fractional variation of the bubble diameter	

d_{C}	Column diameter	m
d_{h}	Diameter of the sparger hole	m
D	Axial dispersion coefficient	$\mathrm{m^2 s^{-1}}$
$\mathrm{Err}D_{\mathrm{G}}$	Percentual error in the calculated axial gas dispersion value caused by an error in the bubble rise velocity value	%
$\mathrm{Dev}D_{\mathrm{G}}$	Percentual deviation of the axial gas dispersion coefficient caused by axial dispersion model's assumptions	%
D_{G}^{+}	Value of the axial gas dispersion coefficient corresponding to the minimum amplitude damping	
$\overline{D}_{\mathrm{G}}$	Average axial gas dispersion coefficient	$\mathrm{m^2 s^{-1}}$
$\widehat{D}_{\mathrm{G}}$	Fractional variation of the axial gas dispersion coefficient	
f	Modulation frequency	Hz
F_1	Parameter defined in Equation 61	$\mathrm{s\ m^{-3}}$
F_2	Parameter defined in Equation 62	$\mathrm{m^{-1}}$
g	Gravitational acceleration	$\mathrm{m\ s^{-2}}$
g	Gravitational acceleration	$\mathrm{m\ s^{-2}}$
H	Coefficient defined as $H = \sqrt[5]{\frac{3}{\pi^2 g}\left(\frac{81}{16}\bar{C}_D + 9\alpha\right)}$	$\mathrm{m^{-\frac{1}{5}}\ s^{\frac{2}{5}}}$
K	Coefficient defined as $K = \sqrt{1 + C_2 D_G^2}$	
J_{D}	Dispersion flux per unit of the column sectional area	$\mathrm{m\ s^{-1}}$
n_{f}	Number of holes in the sparger	
x	Axial distance from the sparger	m
Δx	Axial distance between the measurement points	m
Δx^{+}	Value of the axial distance between the measurement points corresponding to the minimum amplitude damping	m
Q	Gas flow rate from a single sparger hole	$\mathrm{m^3 s^{-1}}$
$\overline{\mathrm{Q}}$	Average gas flow rate from a single sparger hole	$\mathrm{m^3 s^{-1}}$

$\widehat{\mathrm{Q}}$	Fractional variation of the gas flow rate from a single sparger hole	
Re	Reynolds number (ratio of inertial to viscous forces)	
t	Time	s
u	Superficial velocity of the selected phase	m s^{-1}
$\bar{u}_{\mathrm{G}}$	Average gas superficial velocity	m s^{-1}
$\hat{u}_{\mathrm{G}}$	Fractional variation of the gas superficial velocity	
u_{G}^{*}	Bubble rise velocity	m s^{-1}
$\bar{u}_{\mathrm{G}}^{*}$	Average bubble rise velocity	m s^{-1}
$\hat{u}_{\mathrm{G}}^{*}$	Fractional variation of the bubble rise velocity	
Err u_{G}^{*}	Percentual error in the bubble rise velocity value	%
V	Amplitude damping	
Dev$V$	Percentual deviation of the amplitude damping caused by axial dispersion model's assumptions	%

Greek letters

α	Inertial parameter	
ϵ	Gas holdup	
$\bar{\epsilon}$	Average gas holdup	
$\hat{\epsilon}$	Fractional variation of the gas holdup	
μ	Viscosity	Pa s
ρ	Density	kg m^{-3}
σ	Surface tension	N m^{-1}
ω	Angular modulation frequency	rad s^{-1}
ω^{+}	Value of the angular modulation frequency corresponding to the minimum amplitude damping	rad s^{-1}
ϕ	Phase of the gas holdup wave	rad

$\Delta\phi$	Phase-shift	rad
Dev$\Delta\phi$	Percentual deviation of the phase-shift caused by axial dispersion model's assumptions	%

Subscripts

G	Gas phase
L	Liquid phase
max	Maximum value of the variable within the modulation period
min	Minimum value of the variable within the modulation period
x	Evaluated at axial position x

References

[1] W.-D. Deckwer, Bubble column reactors, Wiley New York, 1992.

[2] M.V. Kantak, R.P. Hesketh, B.G. Kelkar, Effect of Gas and Liquid Properties on Gas-Phase Dispersion in Bubble-Columns, Chem Eng J Bioch Eng 59 (1995) 91-100.

[3] M. Baird, R. Rice, Axial dispersion in large unbaffled columns, The Chemical Engineering Journal 9 (1975) 171-174.

[4] E. León-Becerril, A. Liné, Stability analysis of a bubble column, Chemical Engineering Science 56 (2001) 6135-6141.

[5] J.B. Joshi, Gas phase dispersion in bubble columns, The Chemical Engineering Journal 24 (1982) 213-216.

[6] A. Döß, M. Schubert, A. Bieberle, U. Hampel, Non-invasive determination of gas phase dispersion coefficients in bubble columns using periodic gas flow modulation, Chemical Engineering Science 171 (2017) 256-270.

[7] U. Hampel, Anordnung und Verfahren zur Dispersionsmessung sowie Mehrphasenapparat mit einer solchen Anordnung. Patent DE 10 2014 118 649 B3 2015.12.24., 2015.

[8] J. Heijnen, K. Van't Riet, Mass transfer, mixing and heat transfer phenomena in low viscosity bubble column reactors, The Chemical Engineering Journal 28 (1984) B21-B42.

[9] S.B. Kumar, D. Moslemian, M.P. Duduković, Gas-holdup measurements in bubble columns using computed tomography, AIChE Journal 43 (1997) 1414-1425.

[10] K. Loubière, G. Hébrard, P. Guiraud, Dynamics of bubble growth and detachment from rigid and flexible orifices, The Canadian Journal of Chemical Engineering 81 (2003) 499-507.

[11] P. Snabre, F. Magnifotcham, I. Formation and rise of a bubble stream in a viscous liquid, The European Physical Journal B-Condensed Matter and Complex Systems 4 (1998) 369-377.

[12] H.N. Oguz, A. Prosperetti, Dynamics of bubble growth and detachment from a needle, Journal of Fluid Mechanics 257 (1993) 111-145.

[13] W.L. Haberman, R.K. Morton, An experimental study of bubbles moving in liquids, Trans. ASCE 2799 (1954) 227-252.

[14] H. Hikita, H. Kikukawa, Gas Holdup in Bubble Columns. Effect of Liquid Properties, Bull. Univ. Osaka Prefect. Ser. A 22 (1973) 151-160.

[15] K. Mangartz, T. Pilhofer, Untersuchungen zur Gasphasendispersion in Blasensäulenreaktoren, Verfahrenstechnik 14 (1980).

[16] H.F. Bach, T. Pilhofer, Einfluß verschiedener Stoff - und Betriebsgrößen auf den relativen Gasgehalt in Blasensäulen, Chem. Ing. Tech. 49 (1977).